# Tensor network state methods in material science and ab initio quantum chemistry

Örs Legeza

Strongly Correlated Systems "Lendület" Research Group

Wigner Research Centre for Physics, Budapest, Hungary

Workshop II: Tensor Network States and Applications

IPAM-2021, 22.04.2021

# DMRG provides state-of-the-art results in many fields

$$\mathcal{H} = \sum_{ij\alpha\beta} T_{ij}^{\alpha\beta} c_{i\alpha}^{\dagger} c_{j\beta} + \frac{1}{2} \sum_{ijkl\alpha\beta\gamma\delta} V_{ijkl}^{\alpha\beta\gamma\delta} c_{i\alpha}^{\dagger} c_{j\beta}^{\dagger} c_{k\gamma} c_{l\delta} \, ,$$

- $T_{ij}$ kinetic and on-site terms, $V_{ijkl}$ two-particle scatterings
- We consider usually lattice models in real space (DMRG)
- In quantum chemistry sites are electron orbitals (QC-DMRG)
- In UHF QC spin-dependent inetractions (UHF-QCDMRG)
- In relativistic quantum chemistry sites are spinors (4c-DMRG)
- In nuclear problems sites are proton/neutron orbitals (JDMRG)
- In k-space representation sites are momentum eigenstates (k-DMRG)
- For particles in confined potential sites $\rightarrow$ Hermite polynoms
- Major aim: to obtain the desired eigenstates of $\mathcal{H}$.

• Symmetries: Abelian and non-Abelian quantum numbers, double groups, complex integrals, quaternion sym. etc

• # of block states: 1 000 – 60 000. Size of Hilbert space up to $10^8$.

• In ab inito DMRG the CAS size is: 70 electrons on 70 orbitals.

• 1-BRDM and 2-BRDM can be extracted.

# Tensor product approximation

State vector of a quantum system in the discrete tensor product spaces

$$|\Psi_\gamma\rangle = \sum_{\alpha_1=1}^{q_1} \dots \sum_{\alpha_d=1}^{q_d} U(\alpha_1, \dots, \alpha_d, \gamma)\, |\alpha_1\rangle \otimes \cdots \otimes |\alpha_d\rangle \in \bigotimes_{i=1}^{d} \Lambda_i := \bigotimes_{i=1}^{d} \mathbf{C}^{q_i} \ ,$$

where $span\{|\alpha_i\rangle : \alpha_i = 1, \dots, q_i\} = \Lambda_i = \mathbf{C}^{q_i}$ and $\gamma = 1, \dots, m$.

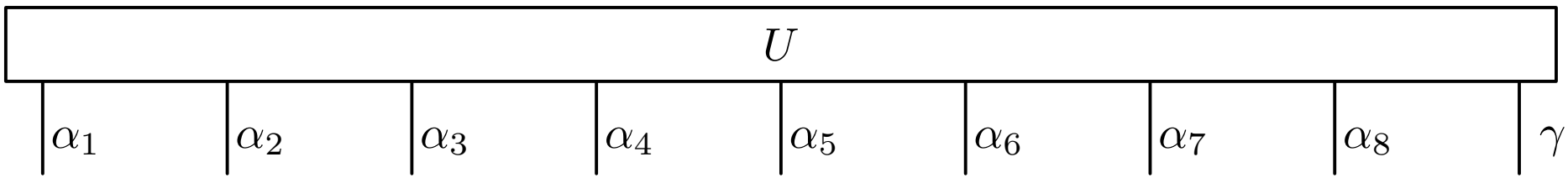


- In a spin-1/2 model $\alpha_i \in \{\downarrow, \uparrow\}$.
- In a spin-1/2 fermionic model $\alpha_i \in \{0, \downarrow, \uparrow, \uparrow\downarrow\}$.

$\dim \mathcal{H}_d = \mathcal{O}(q^d)$ Curse of dimensionality!

- We seek to reduce computational costs by parametrizing the tensors in some data-sparse representation.

# Tensor product representation

- A general tensor network representation of a tensor of order 5.

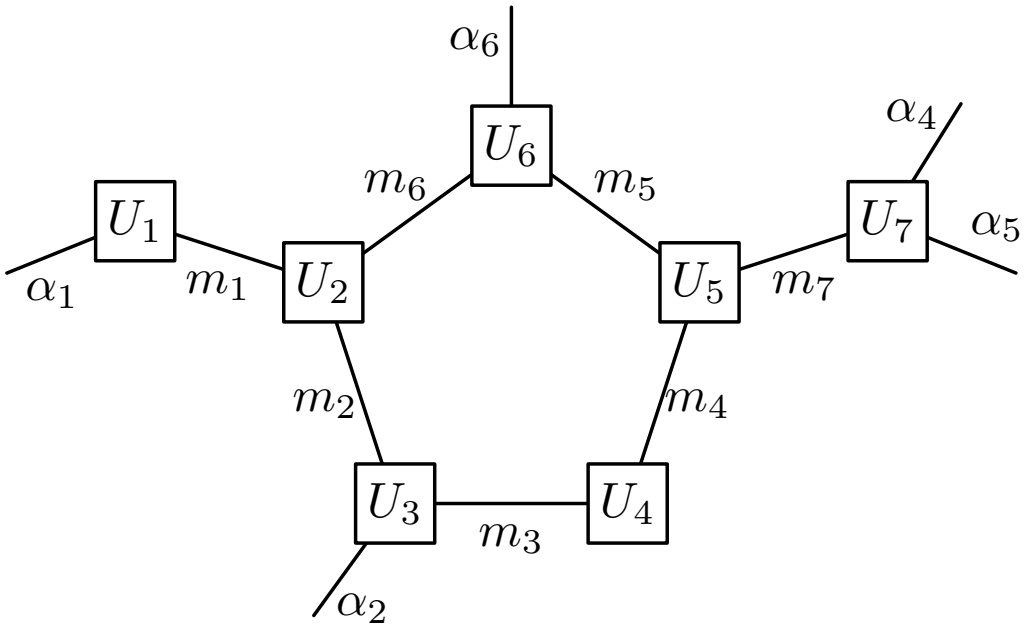


- An arbitrary example of a tensor tree (loop free).

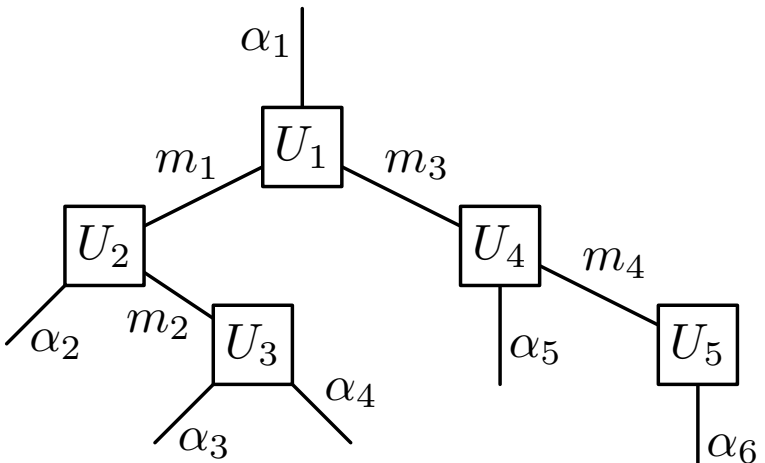

# Matrix product state (MPS) representation / DMRG /TT

• A tensor of order 5 in Matrix Product State (MPS) representation. Also know as Tensor Train (TT).

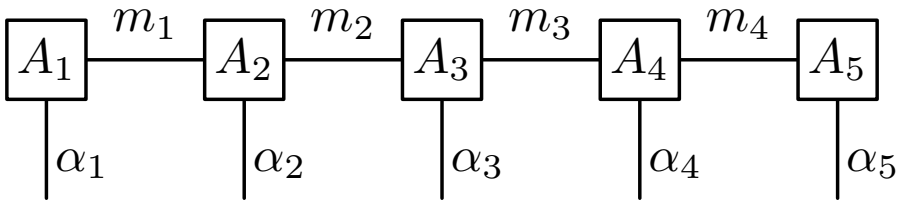


• The tensor $U$ is given element-wise as

$$U(\alpha_1, \ldots, \alpha_d) = \sum_{m_1=1}^{r_1} \cdots \sum_{m_{d-1}=1}^{r_{d-1}} A_1(\alpha_1, m_1) A_2(m_1, \alpha_2, m_2) \cdots A_d(m_{d-1}, \alpha_d).$$

• We get $d$ component tensors of order 2 or 3 which yields a chain of matrix products:

$$U(\alpha_1, \ldots, \alpha_d) = \mathbf{A}_1(\alpha_1)\mathbf{A}_2(\alpha_2) \cdots \mathbf{A}_{d-1}(\alpha_{d-1})\mathbf{A}_d(\alpha_d)$$

with $[\mathbf{A}_i(\alpha_i)]_{m_{i-1}, m_i} := A_i(m_{i-1}, \alpha_i, m_i) \in \mathbb{C}^{r_{i-1} \times r_i}$.

• Ranks ($m_i$) must be controlled.

Redundancy:
$U(\alpha_1, \ldots, \alpha_d) = \mathbf{A}_1(\alpha_1)\mathbf{G}\mathbf{G}^{-1}\mathbf{A}_2(\alpha_2) \cdots \mathbf{A}_{d-1}(\alpha_{d-1})\mathbf{A}_d(\alpha_d)$

# Matrix product state (MPS) representation / DMRG /TT

• A tensor of order 5 in Matrix Product State (MPS) representation. Also know as Tensor Train (TT).

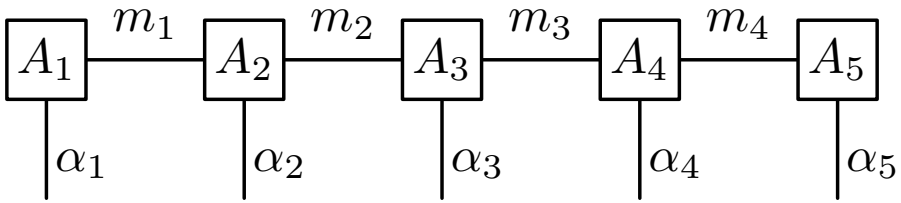


• The tensor $U$ is given element-wise as

$$U(\alpha_1, \ldots, \alpha_d) = \sum_{m_1=1}^{r_1} \ldots \sum_{m_{d-1}=1}^{r_{d-1}} A_1(\alpha_1, m_1) A_2(m_1, \alpha_2, m_2) \cdots A_d(m_{d-1}, \alpha_d).$$

• We get $d$ component tensors of order 2 or 3 which yields a chain of matrix products:

$$U(\alpha_1, \ldots, \alpha_d) = \mathbf{A}_1(\alpha_1)\mathbf{A}_2(\alpha_2) \cdots \mathbf{A}_{d-1}(\alpha_{d-1})\mathbf{A}_d(\alpha_d)$$

with $[\mathbf{A}_i(\alpha_i)]_{m_{i-1}, m_i} := A_i(m_{i-1}, \alpha_i, m_i) \in \mathbb{C}^{r_{i-1} \times r_i}$.

• Ranks ($m_i$) must be controlled.

Affleck, Kennedy, Lieb, Tasaki (87); Fannes, Nachtergale, Werner (91), White (92), Römmer, Ostlund (94); Vidal (03); Verstraete (04); Oseledets, Tyrtyshnikov, (09)

# Extension of MPS to higher dimensional cases: PEPS

White, Noack (1996), Verstraete, Cirac, Murg (2004)

- For 2D systems MPS representation is not optimal
- Short range interactions become also long range

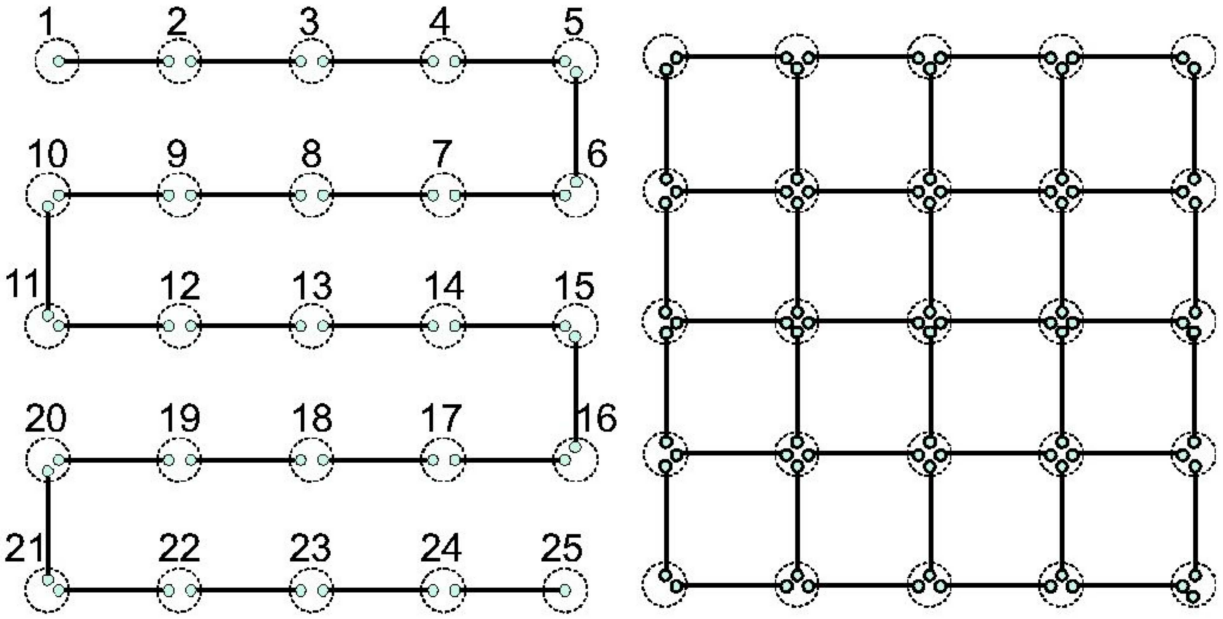


- Entanglement in all 4 direction $\rightarrow$ tensor product states needed!
- Use tensors $A^i[\alpha]_{m_1,m_2,m_3,m_4}$
- Projected Entangled-Pair State (PEPS)

# Higher dimensional loop-free networks (Ex.: Tree-TNS)

Corboz, Vidal (2009), Murg, Verstraete, Ö.L, Noack (2010, 2014), Nakatani, Chan (2013)

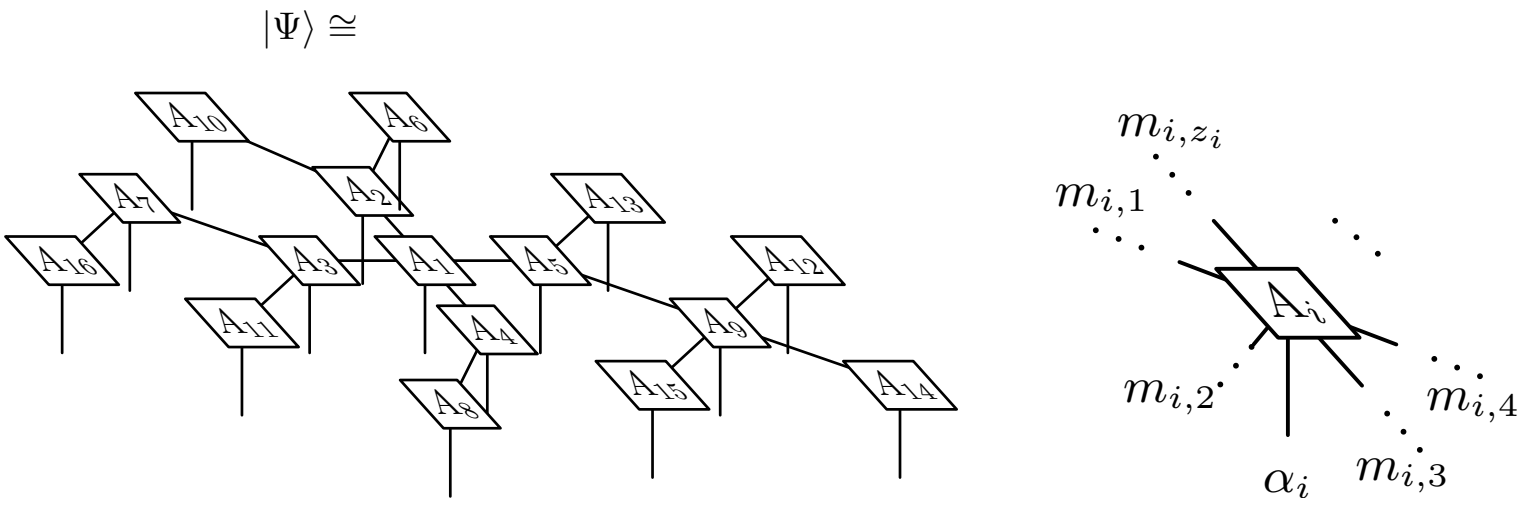


Schematic plot of a higher dimensional network, for example, the tree tensor network state (TTNS). Each node is represented by a tensor $A_i$ of order $z_i + 1$, with $z_i$ is a site dependent coordination number.

- The network supposed to reflect the entanglement structure of the molecule as much as possible.

- Maximal distance between two sites, $2\Delta$, scales logarithmically with $d$ for $z > 2$.
- Expected crossover between MPS and TTNS: one step scales as $D^{z+1}$, while $z = 1$ for the boundary sites

# T3NS a new tensor format Gunst, Verstraete, Wooters, Ö.L., van Neck (2018)

(a)

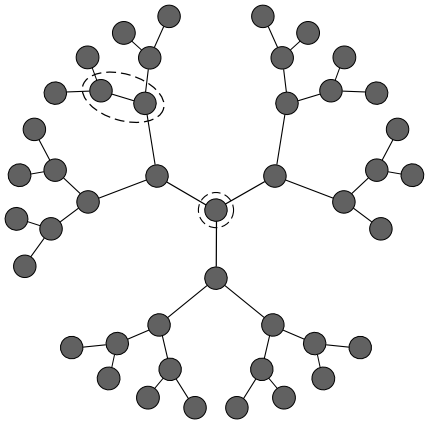

(b)

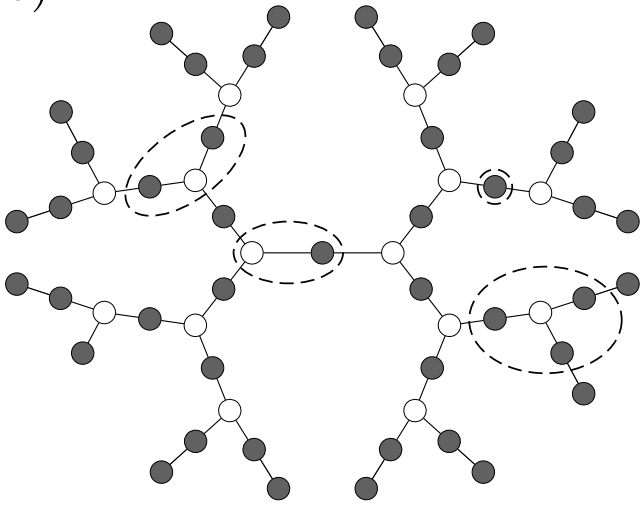

LiF

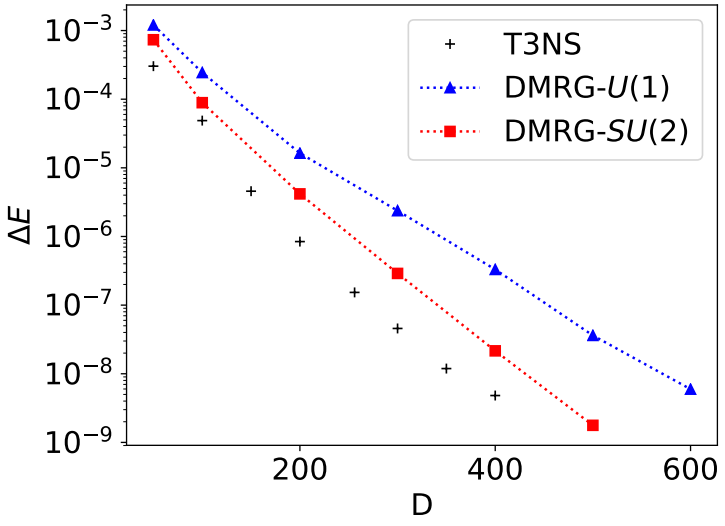


$N_2$

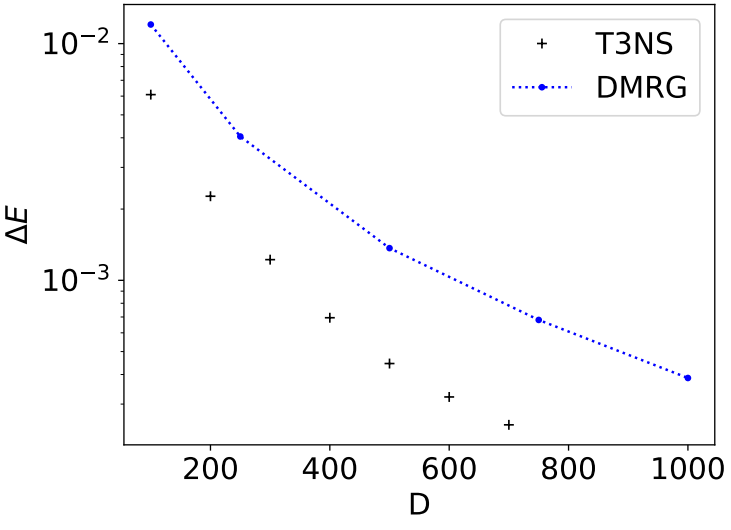

# Resource requirements and complexity

| | DMRG | T3NS |
|---|---|---|
| CPU time: | $\mathcal{O}\left(k^4D^2 + \underline{k^3D^3}\right)$ | $\mathcal{O}\left(k^5D^2 + \underline{k^3D^4}\right)$ |
| Memory: | $\mathcal{O}\left(k^2D^2\right)$ | $\mathcal{O}\left(k^2D^2 + kD^3\right)$ |
| Disk: | $\mathcal{O}\left(k^3D^2\right)$ | $\mathcal{O}\left(k^3D^2 + kD^3\right)$ |

- k : number of orbitals
- D: bond dimension
- The underlined terms correspond with the complexity of the most intensive part of the algorithm, i.e. the matrix-vector product used in the iterative solver.

# One- ($\rho_i$) and two-orbital ($\rho_{i,j}$) reduced density matrix

$$|\psi\rangle = \sum_{\alpha_1,\ldots,\alpha_N} C_{\alpha_1,\ldots,\alpha_N} |\alpha_1 \ldots \alpha_N\rangle \ ,$$

- $\rho_{i,j}$ is calculated by taking the trace of $|\Psi\rangle\langle\Psi|$ over all local bases except for $\alpha_i$ and $\alpha_j$, the bases of sites $i$ and $j$, i.e.,

$$\rho_{i,j}([\alpha_i, \alpha_j], [\alpha_i', \alpha_j']) = \sum_{\substack{\alpha_1,\ldots,\cancel{\alpha_i},\ldots,\\ \cancel{\alpha_j},\ldots,\alpha_N}} C_{\alpha_1,\ldots,\alpha_i,\ldots,\alpha_j,\ldots,\alpha_N} \ C^*_{\alpha_1,\ldots,\alpha_i',\ldots,\alpha_j',\ldots,,\alpha_N} \ .$$

- In the MPS representation, calculation of $\rho_{ij}$ corresponds to the contraction of the network except at sites $i$ and $j$.

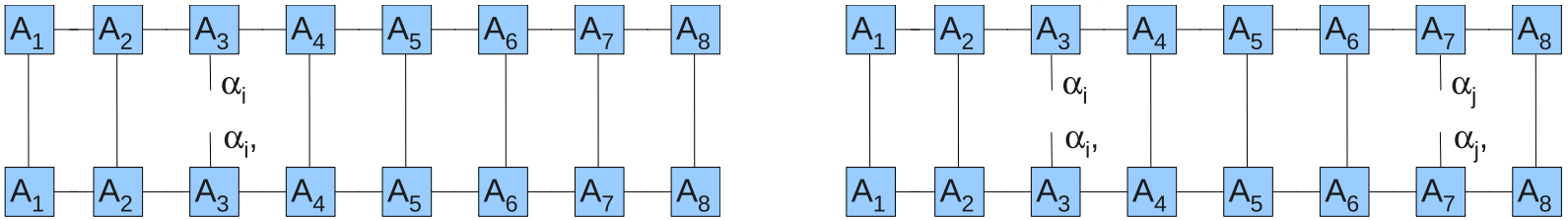


- This can be decomposed as a sum of projector operators based on the free variables $\alpha_i$ and $\alpha_j$.
- $\rho_i$ and $\rho_{i,j}$ can be constructed from operators describing transitions between single-site basis states.

# Relative entropy and mutual information

$$COV(A_1, A_2) = \langle A_1 \otimes A_2 \rangle - \langle A_1 \rangle \langle A_2 \rangle = \mathrm{Tr}(\rho_{12} - \rho_1 \otimes \rho_2)(A_1 \otimes A_2)$$

Uncorr: for all $A_1, A_2$ : $COV(A_1, A_2) = 0$ *iff* $\rho_{12} = \rho_1 \otimes \rho_2$

Spec: $\rho_{12} = |\psi_{12}\rangle\langle\psi_{12}| \quad \rightarrow \quad |\psi_{12}\rangle = \sum_i \sqrt{\lambda_i} |\psi_{1,i}\rangle \otimes |\psi_{2,i}\rangle$

Uncorr: $|\psi_{12}\rangle = |\psi_{1,i}\rangle \otimes |\psi_{2,i}\rangle$

Correlation expressed by the state only

$$I_{12}(\rho_{12}) = D(\rho_{12}||\rho_1 \otimes \rho_2) = S(\rho_1) + S(\rho_2) - S(\rho_{12})$$

where

$$D(\rho||\rho') = \mathrm{Tr}\rho(\ln \rho - \ln \rho'), \qquad S(\rho) = -\mathrm{Tr}\rho \ln \rho$$

Spec: $\rho_{12} = |\psi_{12}\rangle\langle\psi_{12}|$

$$I_{12}(\rho_{12}) = S(\rho_1) + S(\rho_2) - S(\rho_{12}) = 2S(\rho_1) = 2S(\rho_2)$$

since

$$S(\rho_{12}) = 0, S(\rho_1) = S(\rho_2)$$

Notion of entanglement, no classical analogue

# Tensor topology optimization: $\sum_{ij} I_{ij} \times d_{ij}^{\eta}$ (Ex. LiF 6/25)

Energetical ordering (MPS) $\quad d_{ij} = |i - j| \quad$ Entanglement localization (MPS)

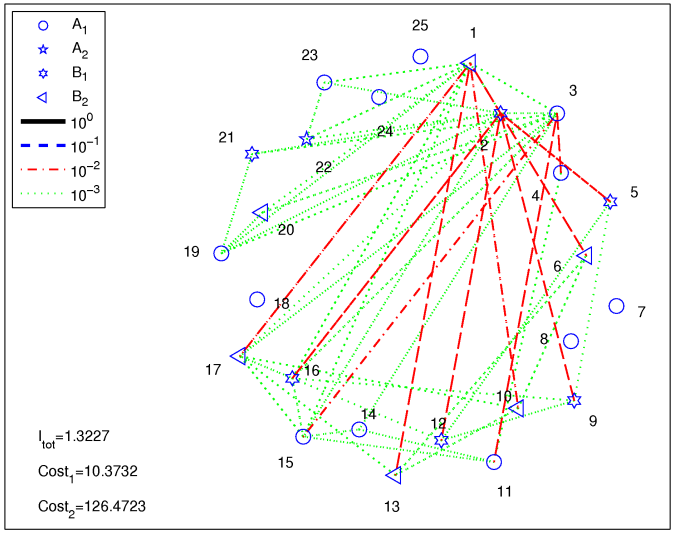


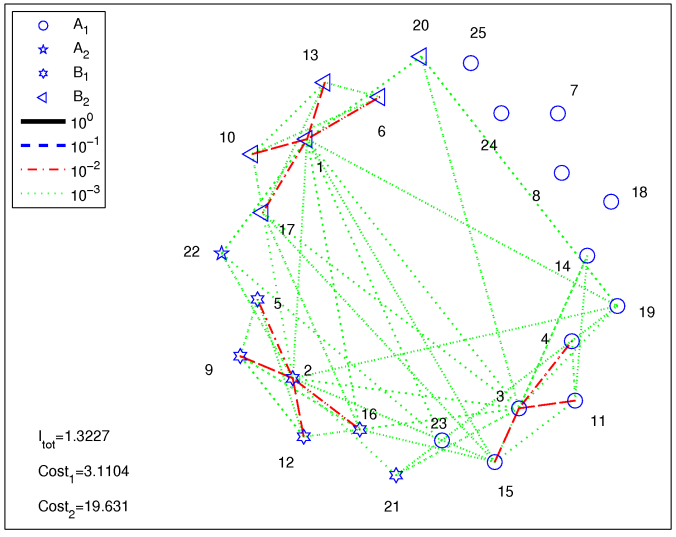


- Reordering orbitals by minimizing the entanglement distance: $\hat{I}_{\text{dist}} = \sum_{i,j} I_{i,j} \times |i - j|^{\eta}$ ,
- Apply spectral graph theory: Fiedler vector $x = (x_1, \ldots x_N)$ is the solution that minimizes $F(x) = x^{\dagger} L x = \sum_{ij} I_{i,j}(x_i - x_j)^2$, with $\sum_i x_i = 0$ and $\sum_i x_i^2 = 1$, and the graph Laplacian is $L = D - I$ with $D_{i,i} = \sum_j I_{i,j}$.
  The second eigenvector of the Laplacian is the Fiedler vector.
- also see recent work of Dupuy and Friesecke

# Change of basis and entanglement (1D Hubbard Model)

Xiang (1996); Nishimoto, Jeckelmann, Gebhard, Noack (2002); Ö.L., Sólyom (2003)

| Entropy behavior: | $U = 0$ | $U = \infty$ |
|---|---|---|
| momentum space: | $I_{\rm Tot} = \sum_p S_p = 0$ | $I_{\rm Tot} = N \ln 4$ |
| real space: | $I_{\rm Tot} = N \ln 4$ | $I_{\rm Tot} = N \ln 2$ |

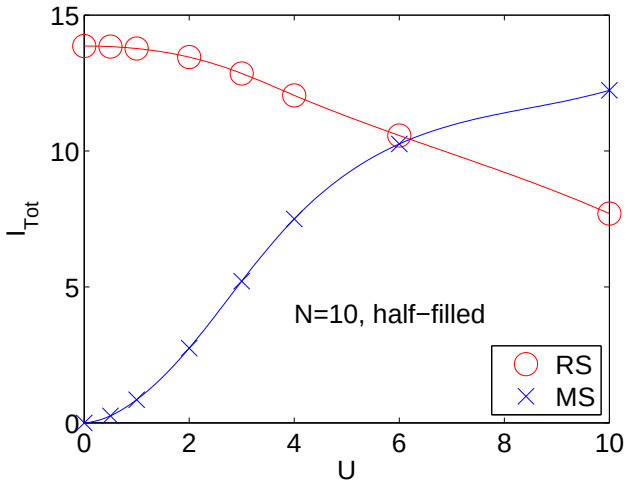


$$\mathcal{H} = -t \sum_{j=1,\sigma}^{N} \left( c^{+}_{j,\sigma} c_{j+1,\sigma} + c^{+}_{j+1,\sigma} c_{j,\sigma} \right) + U \sum_{j=1}^{N} n_{j,\uparrow} n_{j,\downarrow}$$

$\epsilon(k) = \sum_r e^{-ikr} t(r)$, where $k_i = (2\pi n)/N$, $-N/2 < n \leq N/2$

$T_{ij} = -2t \cos(k_i) \delta(i-j)$ and $V_{ijkl} = (U/N) \delta(i+j-k-l)$

$$\mathcal{H} = \sum_{k\sigma} \epsilon_k c^{\dagger}_{k\sigma} c_{k\sigma} + \frac{U}{N} \sum_{pkq} c^{\dagger}_{p-q\uparrow} c^{\dagger}_{k+q\downarrow} c_{k\downarrow} c_{p\uparrow},$$

momentum space exact at $U = 0$, crossover with $U$

# Momentum space: g-ology and entanglement

Ehler, Sólyom, Ö.L., Noack (2015)

$$\mathcal{H} = \sum_{k\sigma} \epsilon_k c^\dagger_{k\sigma} c_{k\sigma} + \frac{U}{N} \sum_{pkq} c^\dagger_{p-q\uparrow} c^\dagger_{k+q\downarrow} c_{k\downarrow} c_{p\uparrow},$$

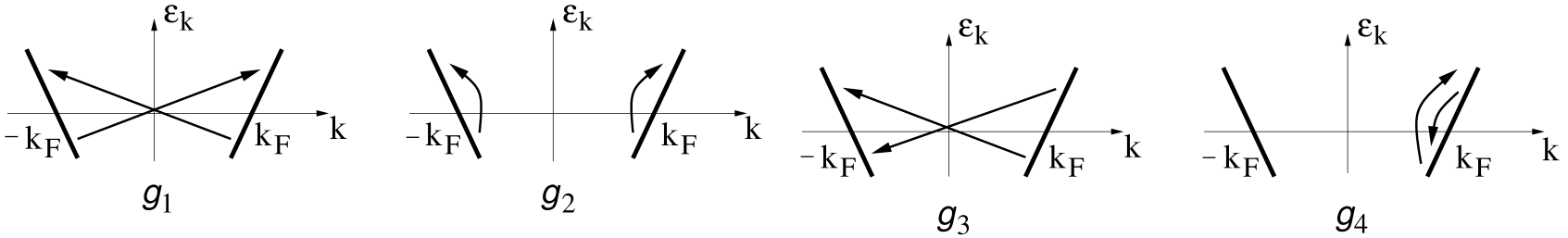


Half-filled

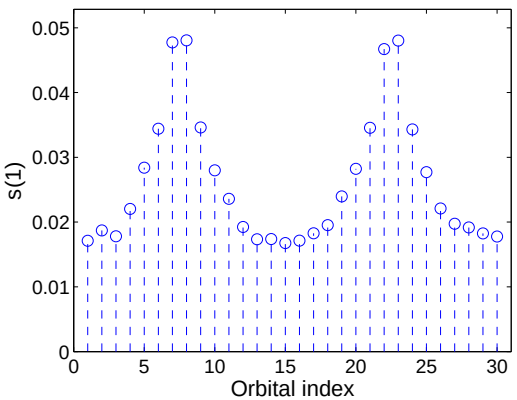


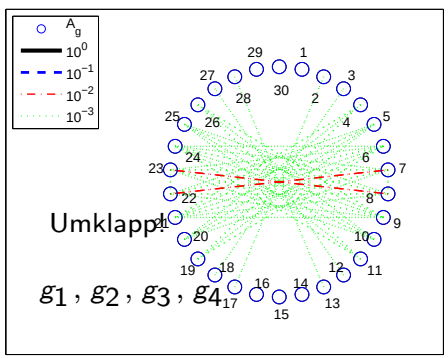


Two holes

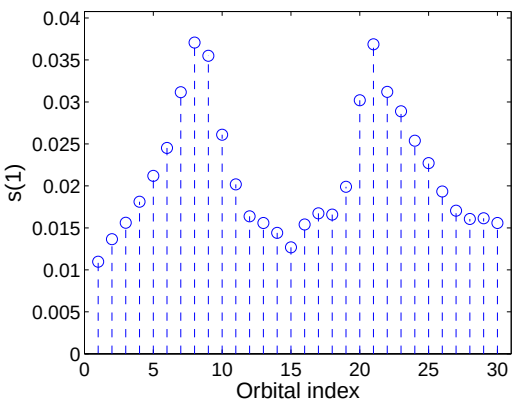


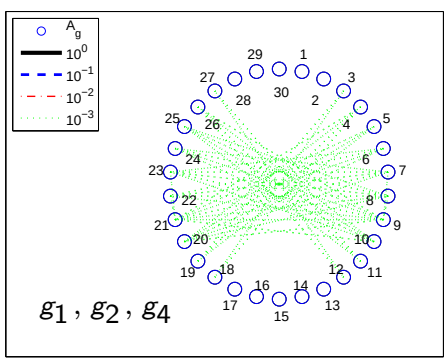

# Basis states transformation applied to the Hamiltonian

Murg, Verstraete, Ö.L., Noack (2010)

$$H = \sum_{ij} T_{ij} c_i^\dagger c_j + \sum_{ijkl} V_{ijkl} c_i^\dagger c_j^\dagger c_k c_l \,,$$

The function $E(U)$ can be expressed as

$$E(U) = \sum_{ij} \tilde{T}(U)_{ij} \langle c_i^\dagger c_j \rangle + \sum_{ijkl} \tilde{V}(U)_{ijkl} \langle c_i^\dagger c_j^\dagger c_k c_l \rangle \text{ with}$$

$$\begin{aligned} \tilde{T}(U) &= U T U^\dagger \\ \tilde{V}(U) &= (U \otimes U) V (U \otimes U)^\dagger. \end{aligned}$$

The correlation functions $\langle c_i^\dagger c_j \rangle$ and $\langle c_i^\dagger c_j^\dagger c_k c_l \rangle$ are calculated with respect to the original state and are not dependent on the parameters in $U$. With the function $E(U)$ in this form, its gradient can be calculated.

Numerically, this was found not stable.

Similarly basis rotation based on the one-particle reduced density matrix
Rissler, Noack, White (2006)

# Redefinition of the fermionic modes by a linear transformation

- Linear transformations of a set of fermionic annihilation operators $\{c_i\}$ to a new set $\{d_i\}$ satisfying the canonical anti-commutation relations:

$$c_i = \sum_{j=1}^{Np} U_{i,j} d_j, \quad p \text{ denotes the number of different fermion species}$$

- Under this change of basis a state vector $|\psi(U)\rangle = G(U)|\psi(\mathbb{1})\rangle$

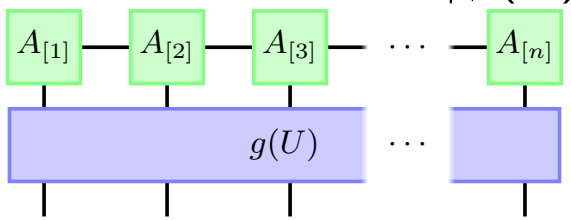


- Denoting the Hamiltonian written in terms of the transformed modes by $H(U) = G(U)^\dagger H G(U)$, we are interested in the solutions of

$$(U_{\text{opt}}, |\psi_{\text{opt}}\rangle) = \operatorname{argmin}_{\substack{U \in U(Np), \\ |\psi\rangle \in \mathcal{M}_{D_{\max}}}} \langle\psi|H(U)|\psi\rangle.$$

- The global basis change is composed of local unitaries solutions of

$$U_{\text{opt}}^{\text{loc}} = \operatorname{argmin}_{U \in V} f_j\big(|\psi(\mathbb{1}_j \oplus U \oplus \mathbb{1}_{N-j-2})\rangle\big),$$

cost function $f_j^{(1)}(|\psi\rangle) = ||\Sigma_\psi^j||_1$ where $\Sigma_\psi^j$ denotes the Schmidt spectrum of $|\psi\rangle$ for a bipartiting cut between sites $j$ and $j+1$.

# Local mode transformation: black-box tool to improve basis

Krumnow, Veis, Ö. L., Eisert, 2014-2016

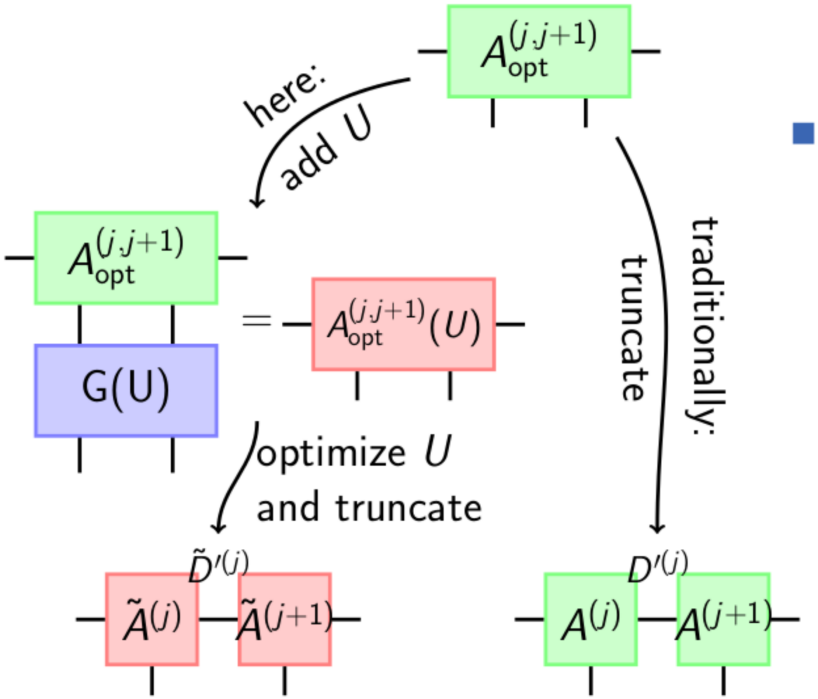


- Update the operators with $U_{\text{global}} := \mathbb{1} \oplus U \oplus \mathbb{1}$
  e.g. the **Hamiltonian**
  $$H \mapsto \tilde{H} := G(U_{\text{global}})\, H\, G^{\dagger}(U_{\text{global}})$$
  exploiting their second quantized representation
  $$H(T, V) \mapsto \tilde{H} = H(\tilde{T}, \tilde{V})$$
  $$T \mapsto \tilde{T} := U_{\text{global}}\, T\, U_{\text{global}}^{\dagger}$$
  $$V \mapsto \tilde{V} := (U_{\text{global}} \otimes U_{\text{global}})\, V\, (U_{\text{global}}^{\dagger} \otimes U_{\text{global}}^{\dagger})$$

- Cost function: $S^{\alpha}(\rho) = \log \mathrm{Tr}\rho^{\alpha}/(1-\alpha)$, predefined accuracy upper bounded by Rényi entropies $\alpha < 1$, using $\alpha = 1/2$ and finding $U_{loc}^{opt}$ by Nelder-Mead method
- We perform mode transformation iteration with finite number of sweeps with fixed bond dimension
- We peform a global reordering in order to avoide being trapped in local minima (Fiedler vector, genetic algorithm)
- Extension to more than two sites is also possible

# Large-scale DMRG results (Ex.: $Be_6$ ring)

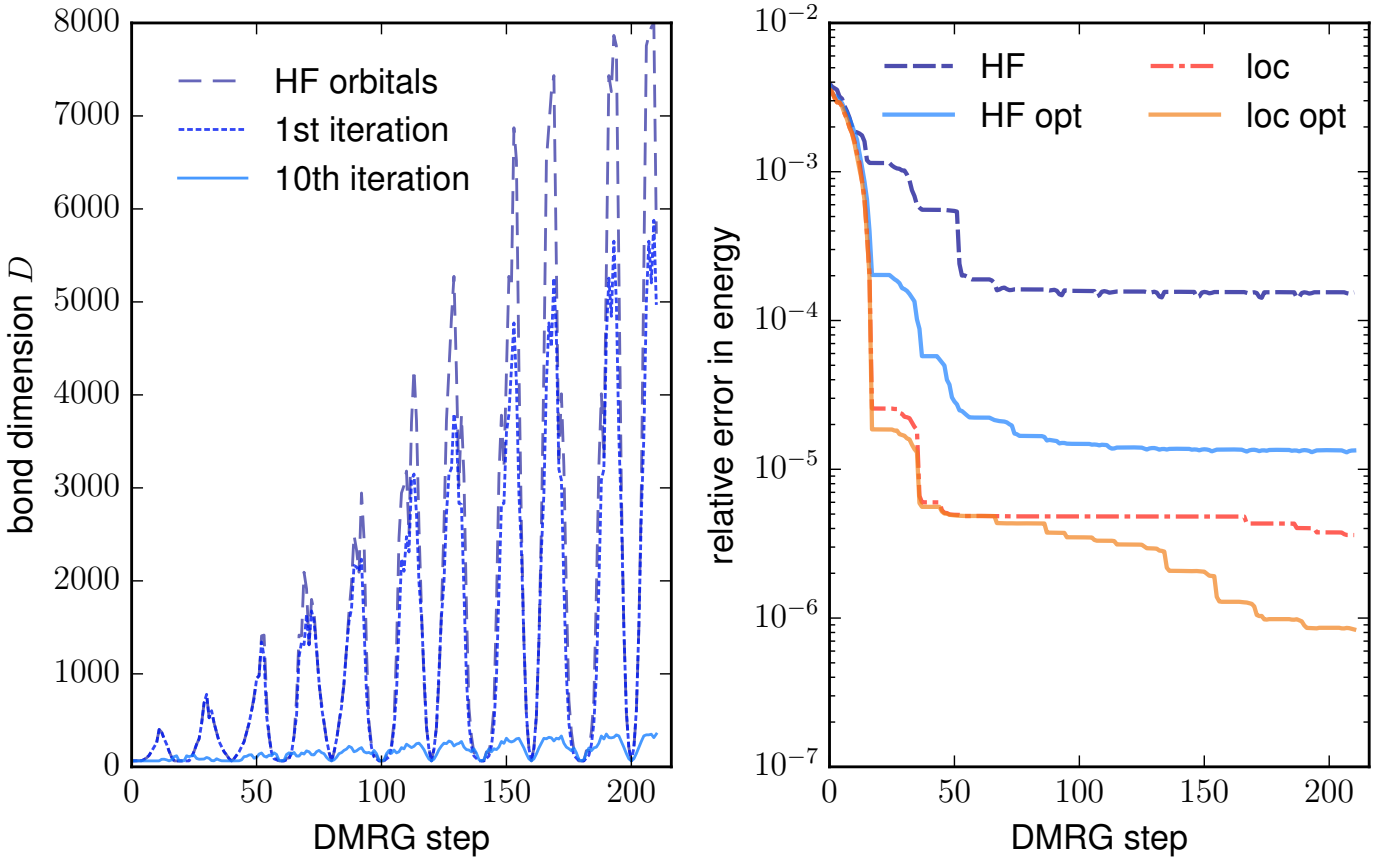


Left panel: bond dimension needed for a bounded truncation error $\epsilon_{trc} \leq 10^{-6}$ and $D_{\text{min}} = 64$ when starting in the HF basis.
Right panel: the relative error in energy $(\langle\psi|H|\psi\rangle - E_0)/E_0$ obtained by calculations with $D_{\text{max}} = 256$.
$E_0$ was obtained from a calculation with $D_{\text{max}} = 2048$ in the localized basis.

# Mode Transformation: $I_{\mathrm{tot}} = \sum_i S(\rho_i),\ I_{\mathrm{overall}} = \sum_{ij} I_{ij}|i-j|^2$

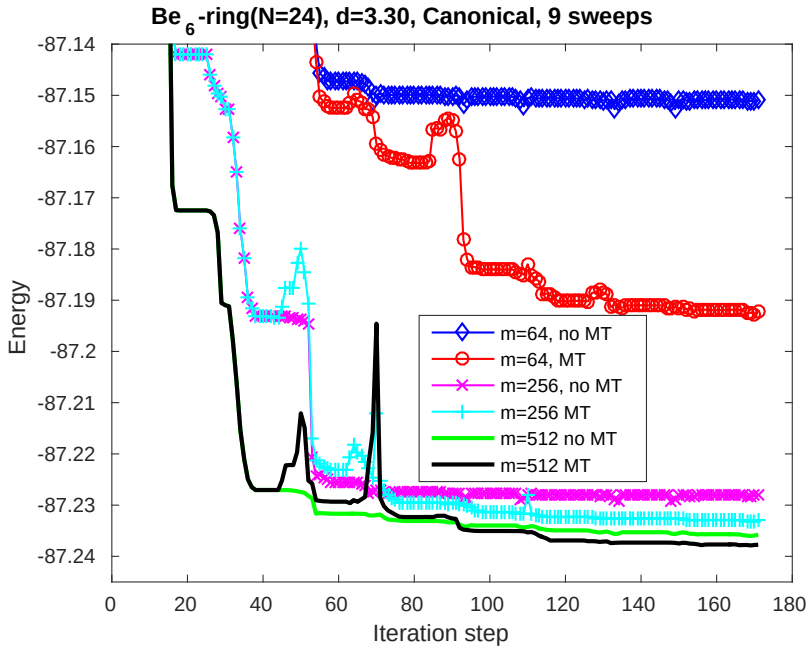


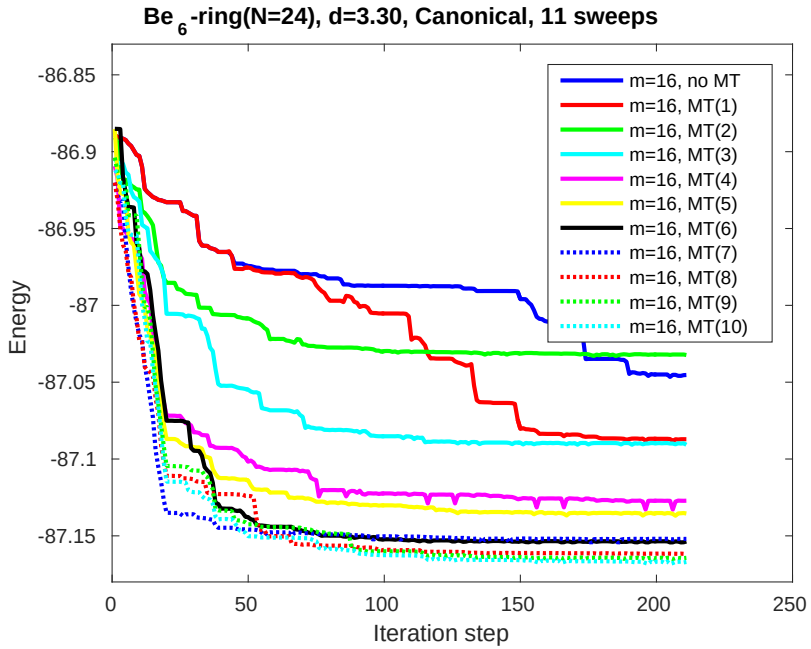


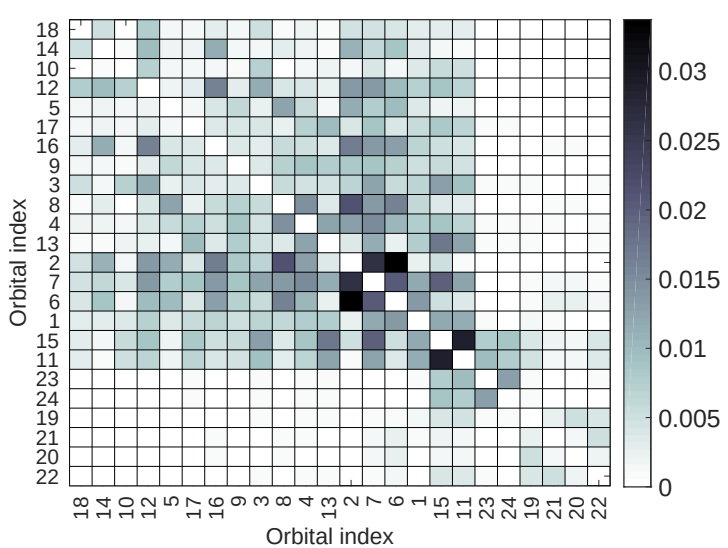


$I_{\mathrm{tot}} = 4.06, I_{\mathrm{overall}} = 211.27$

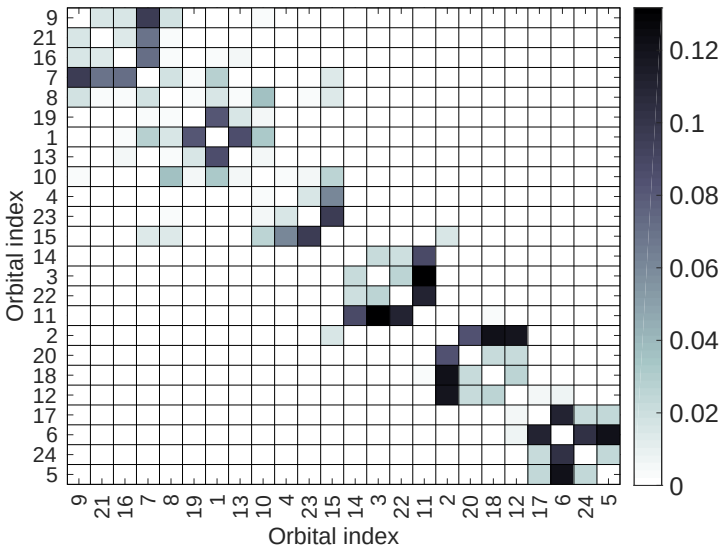


$I_{\mathrm{tot}} = 5.26, I_{\mathrm{overall}} = 42.65$

# 2d spinless fermions with PBCs Krumnow, Veis, Eisert, Ö.L (2019)

$$H = \sum_{\langle i,j \rangle} c_i^\dagger c_j + \sum_{\langle i,j \rangle} V n_i n_j,$$

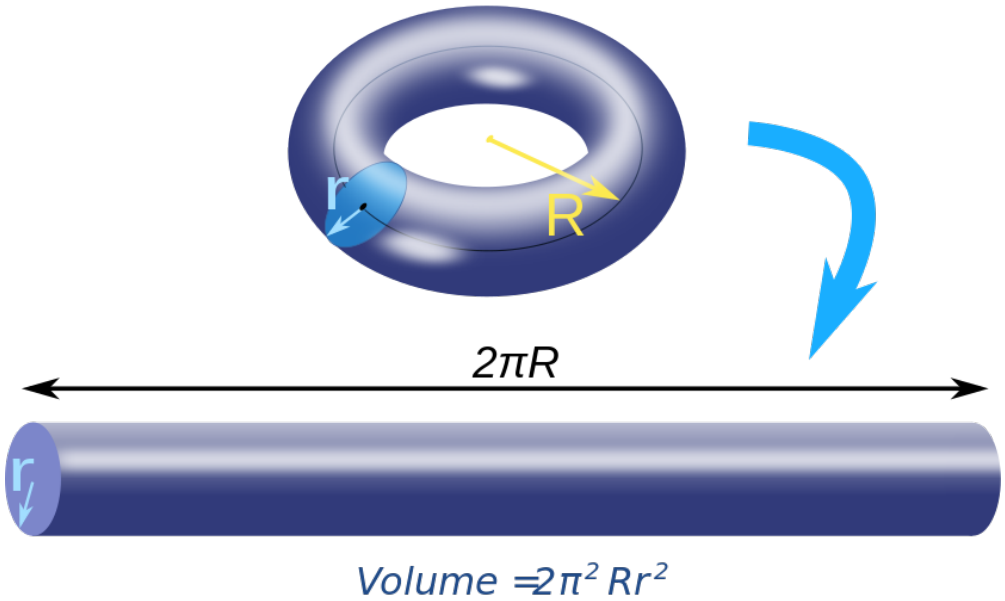


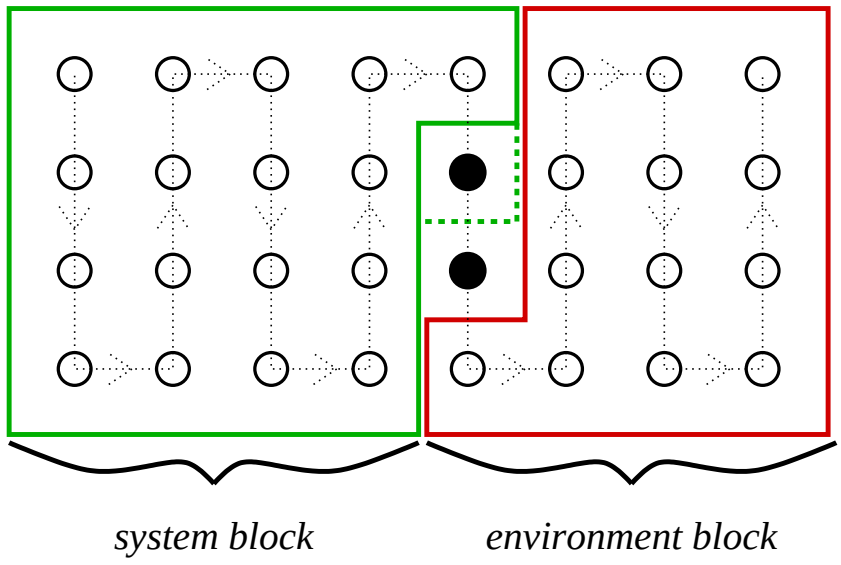


- Optimization on the mps manifold and on the Grassman manifold
- Hamiltionian becomes long ranged

$$H = \sum_{i,j=1}^{n} t_{i,j} c_i^\dagger c_j + \sum_{i,j,k,l=1}^{n} v_{i,j,k,l} c_i^\dagger c_j^\dagger c_k c_l,$$

# 2d spinless fermions on a torus Krumnow, Veis, Eisert, Ö.L (2019)

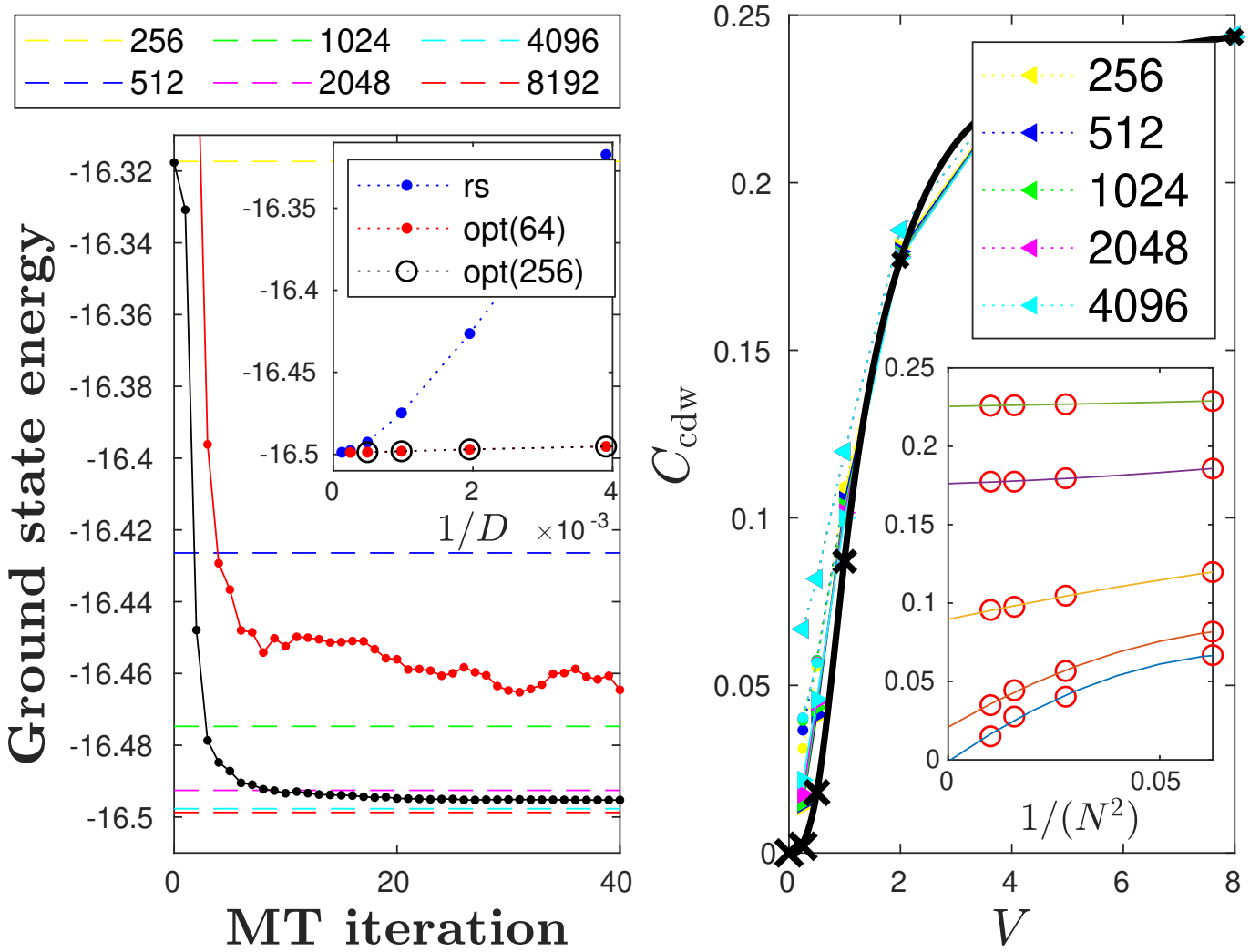


- $C_{\mathrm{cdw}} = (1/N^4) \sum_{i,j} \eta_{i,j} (n_i - 1/2)(n_j - 1/2)$
- One- and two-particle reduced density matrices. $\rho^{(2)}_{i,j,k,l} = \langle c_i^\dagger c_j^\dagger c_k c_l \rangle$
- Torus geometry: faster finize size scaling

# Residual entropy?

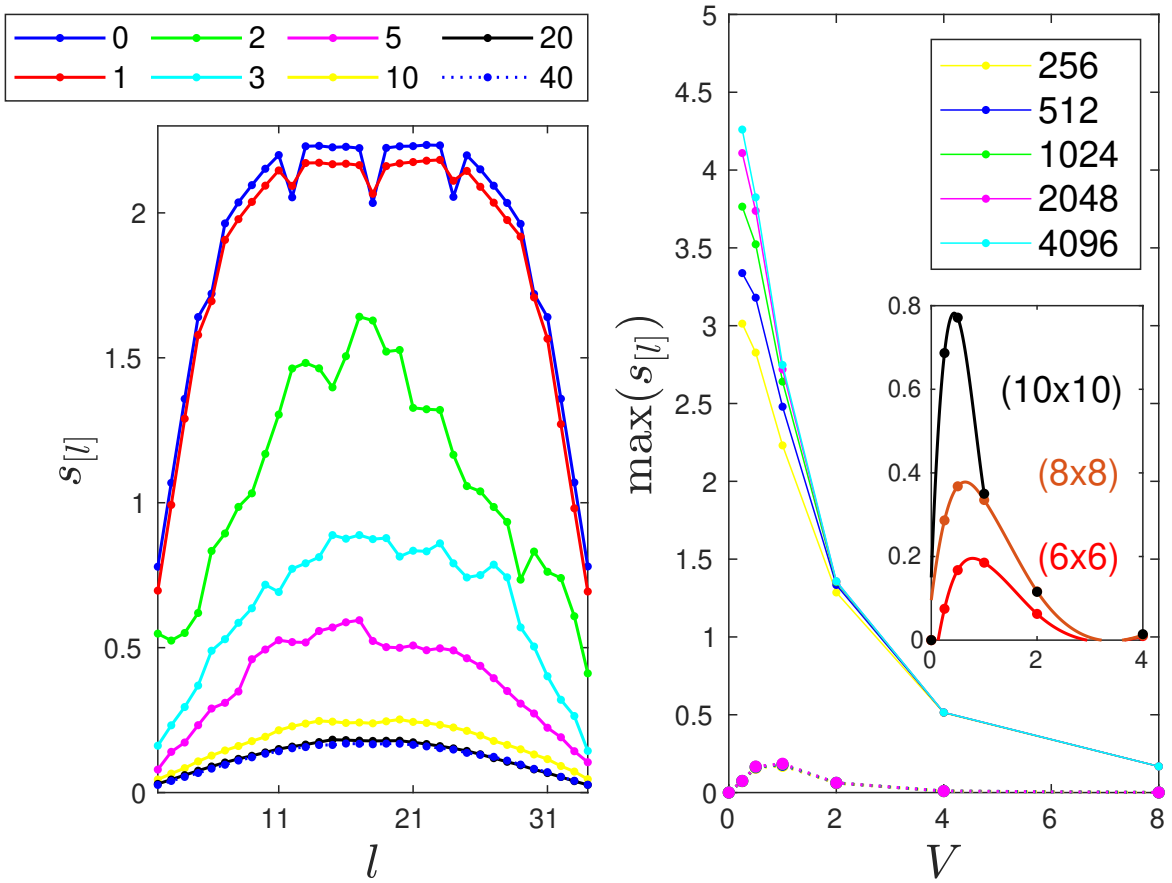


- Maximum of block entropy is reduced by a factor 10 (entropy is a logarithmic function)
- Highly simmetric and smooth entropy profiles is obtained
- $V_c \to 0$ with increasing N
- Scaling of residual entropy, quasi-particle picture etc
- MPO bond dimension increases (use massive parallelization)

# Saturation of half-chain block entropy with $1/D$

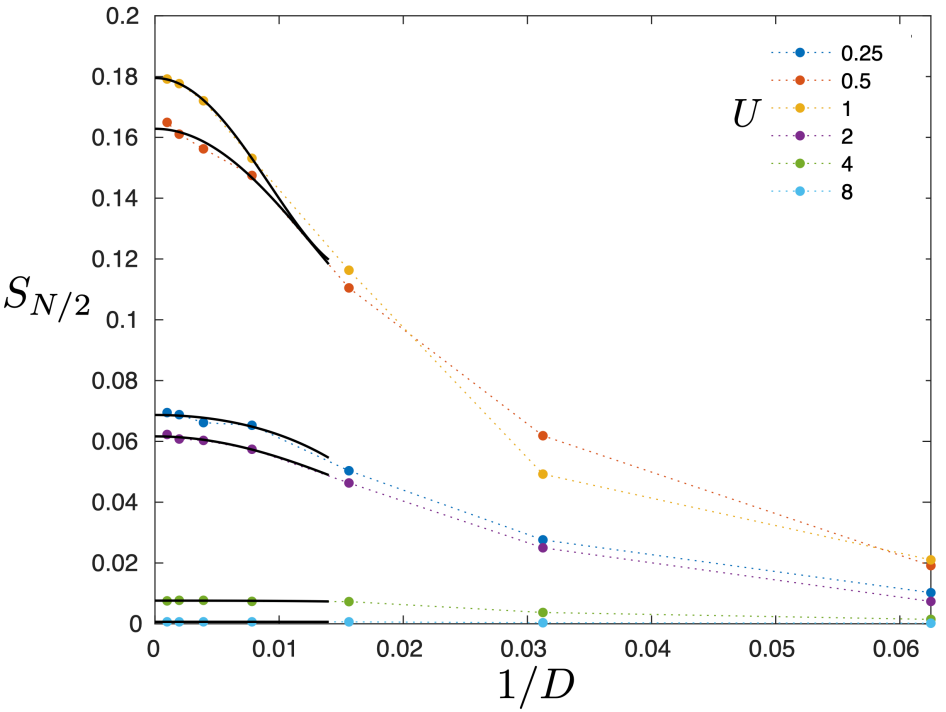


Half-filled, 6x6 lattice

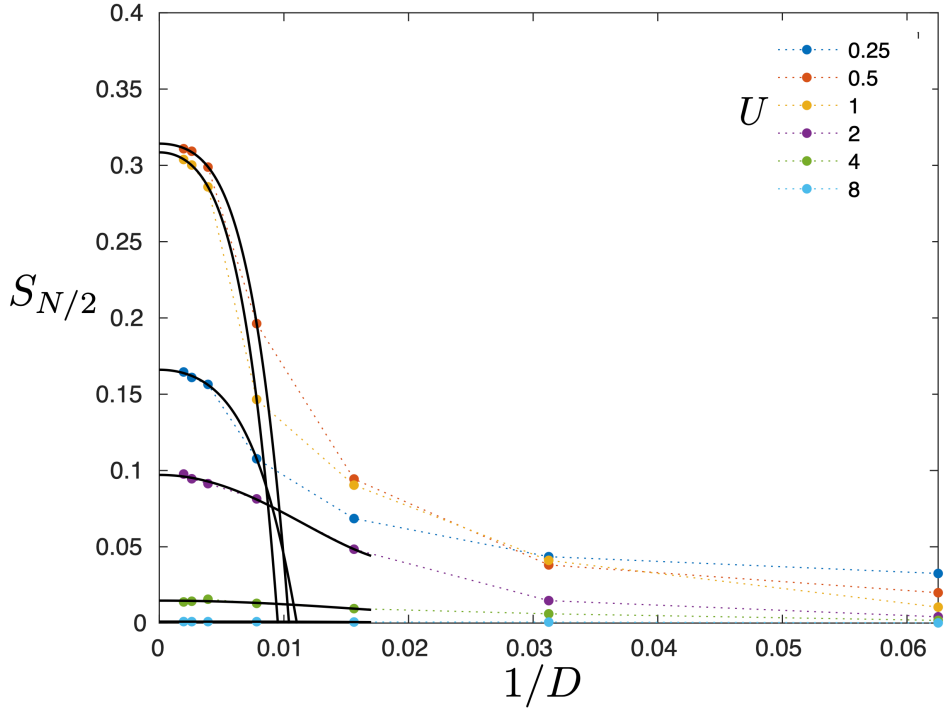


8x8 lattice

- Saturation of block entropy with $1/D$
- Scaling of block entropy with system needs more work
- Higher dimensional networks and mode transformation
- Further applications already to quantum impurity models, 2d Hubbard like models, graphene nanoribbons, Wigner crystals

# Example on graphene nanoribbons I. Hagymási, Ö.L (2016)

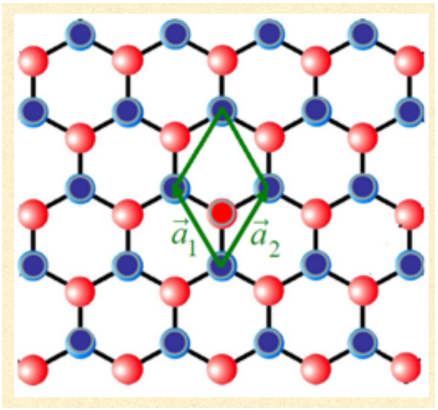


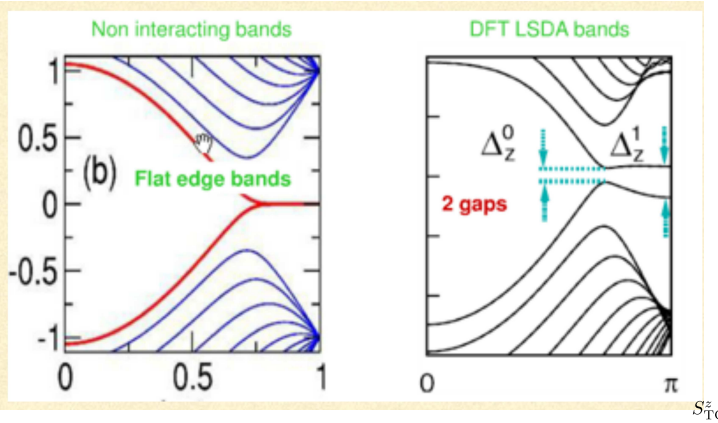


- Flat bands disappear when interaction is switched on
- Need TNS due to strong quantum fluctuations

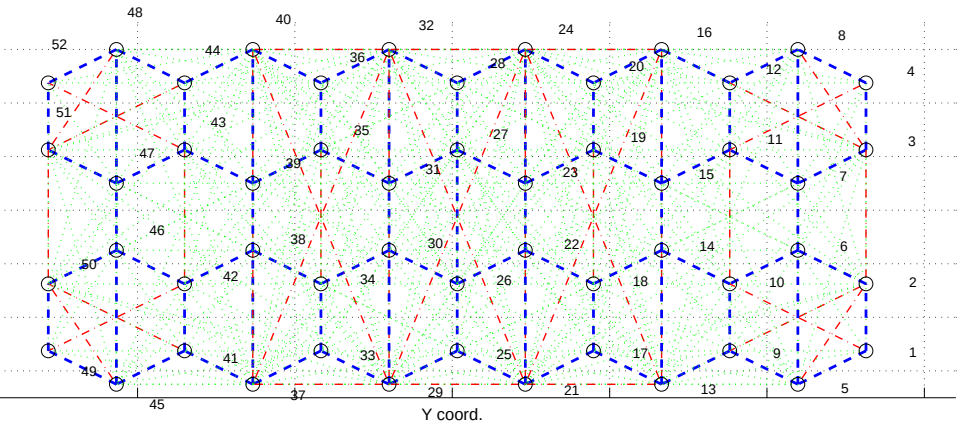


- DMRG $D = 20000$, $U = 2$

Problem revisited with modetransformation, monitoring emerging modes for zigzag, armchair, periodic BC etc.. Fraction of D is needed

Mate, Vizkeleti, Szalay, Hagymasi, Ö.L.

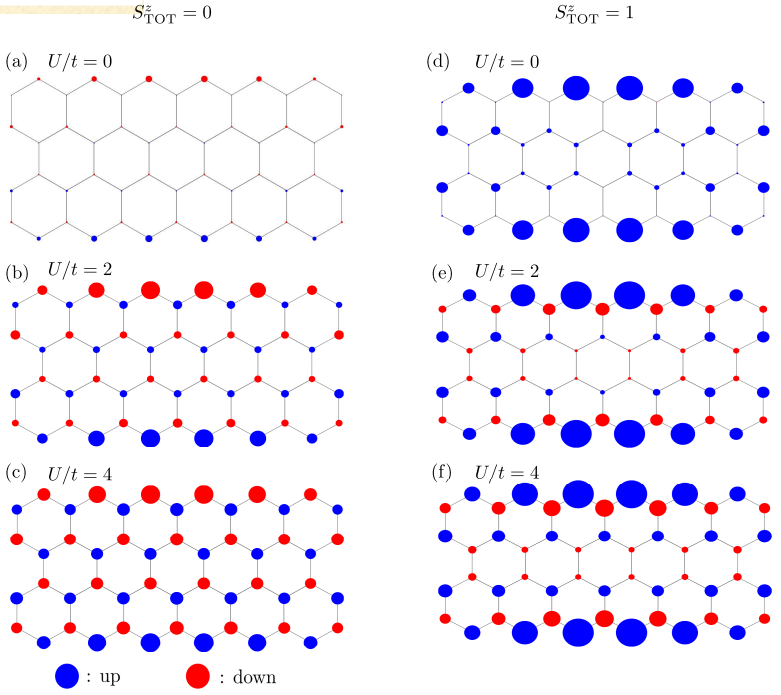


(left) $S_i^z$ for the ground state in the presence of a pinning magnetic field at the bottom zigzag

# Topologically protected, correlated end spin formation in carbon nanotubes Moca, Izumida, Dóra, Ö.L., Zaránd (2019)

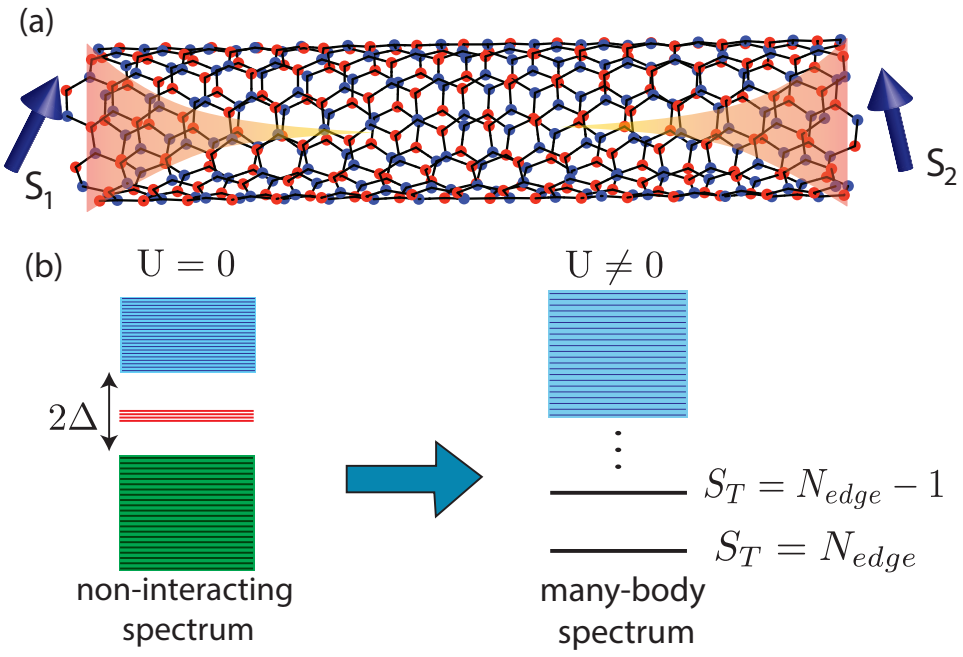


- $S_1 = S_2 = \frac{N_{\rm edge}}{2}$
- Topological nanotubes spontaneously form double dot devices, which may provide a platform for quantum computation.
- Sign of the interaction can be changed by changing the dielectric constant of the environment.
- Coupling between ferromagnetic edge states is length and chirality dependent

# New basis representation $\rightarrow$ quantum chemistry framework

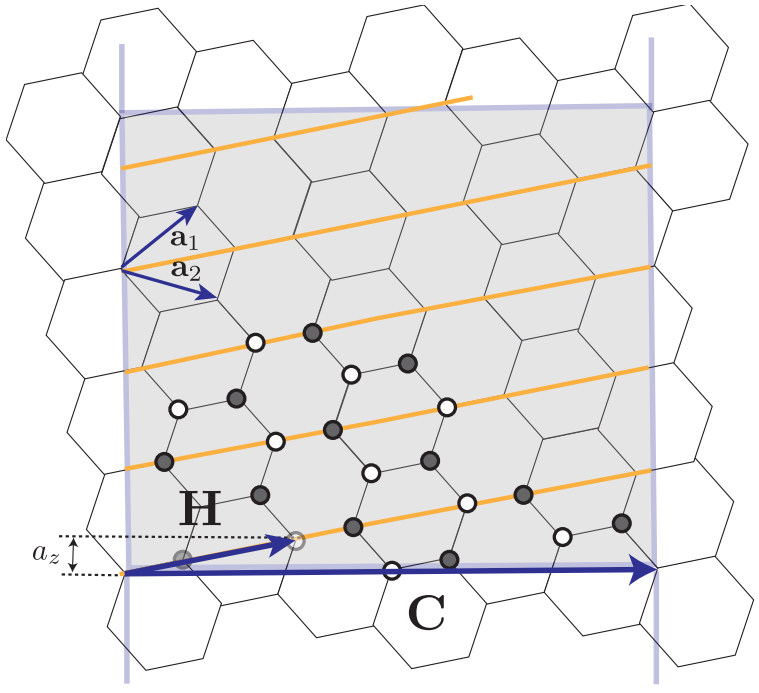


$$H_0 = -\sum_{\mathbf{x},\mathbf{x}',s} t(\mathbf{x}-\mathbf{x}')c_s^\dagger(\mathbf{x})c_s(\mathbf{x}') \;\text{ with }\; \mathbf{r}=\mathbf{r}(\mathbf{x})=\mathbf{r}(\nu,\mathrm{l},\tau)\,,$$

• Construct and diagonalize the non-interacting part of the Hamiltonian and obtain the corresponding eigenfunctions $\phi_\alpha(\mathbf{r}) \equiv \phi_\alpha(\nu,\ell,\tau)$,

•Express the Coulomb interaction in this basis.

•For effective Coulomb interaction we use the so-called Ohno potential,

$$V(\mathbf{r}_1-\mathbf{r}_2) = \frac{e^2}{\epsilon_r}\frac{1}{\sqrt{(\mathbf{r}_1-\mathbf{r}_2)^2+\alpha^2}},\;\;,$$

# Effective exchange interaction $J_{\text{eff}}$ between localized end spins

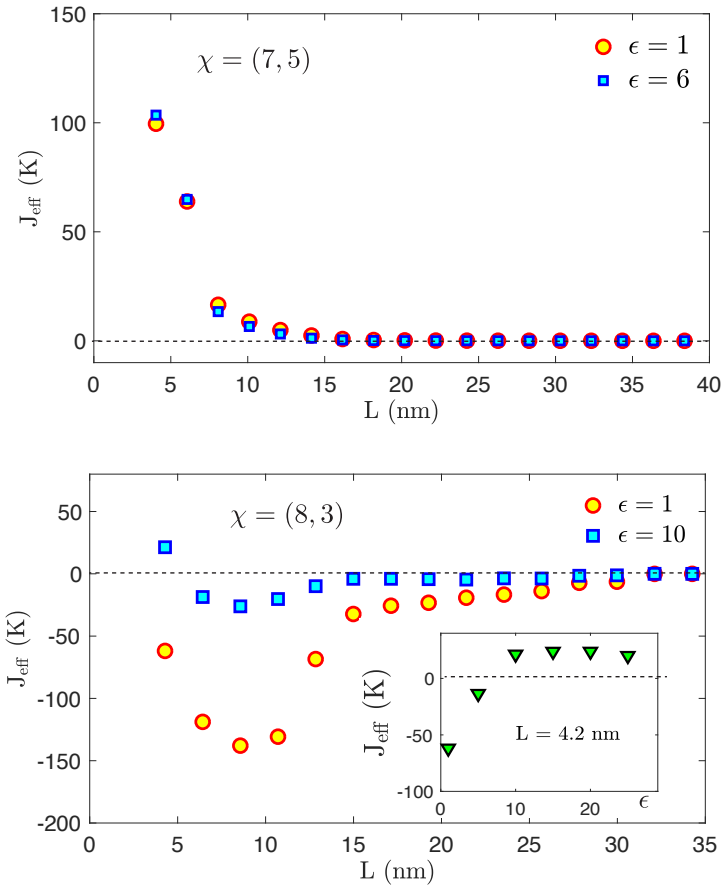


- $J_{\text{eff}}$ between localized end spins as function of its length.
- When $N_{edge}$=1, $J_{eff}$ is always positive indicating an antiferromagnetic exchange
- For $N_{edge} \geq 2$ an antiferromagnetic to ferromagnetic transition occurs.
- For appropriate nanotube length, the sign of the interaction can be changed by changing the dielectric constant of the environment.

# Long time evolution Krumnow, Eisert, Ö.L. (2019)

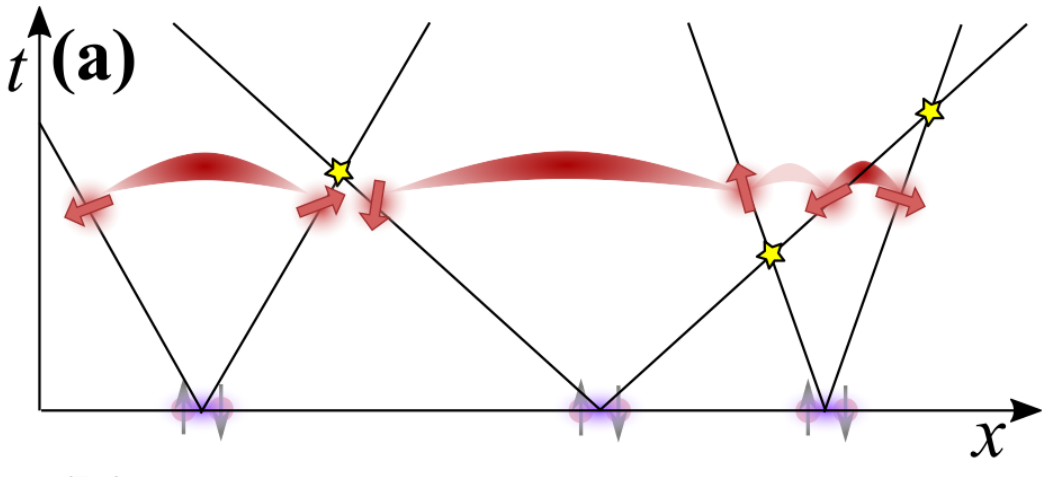


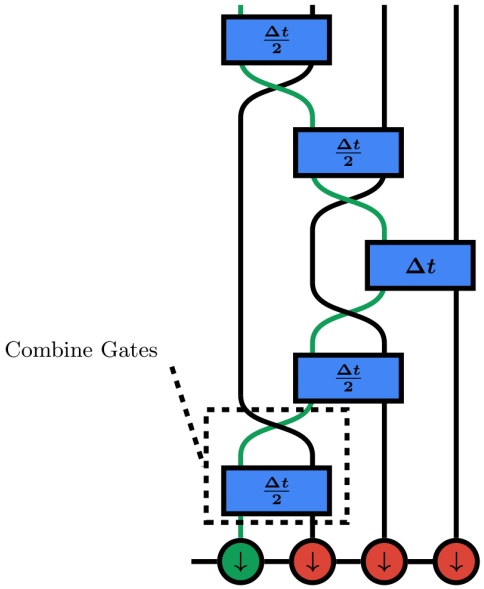


- At time $t = 0$ we perturb the system.
- After the quench the quasiparticles collide with each other.
- There are different time-evolution methods for MPS which are currently in use to solve the time-dependent Schrödinger equation (TDSE).
- application of $\hat{U}(\delta_t) = e^{-i\delta_t \hat{H}}$, i.e. , $|\psi(t)\rangle \rightarrow |\psi(t+\delta_t)\rangle$
- time-evolving block decimation (TEBD), *MPOW*$^{\mathrm{I,II}}$, Krylov, time-dependent variational principle (TDVP)
- each has advatages and disadvateges.
- TDVP $\rightarrow$ general non-local Hamiltonians (quantum chemsitry)

# Long time evolution Krumnow, Eisert, Ö.L. (2019)

- correlations in the system spread and bond dimension increases unboundedly in time
- Combination of time evolution and adaptive mode transformation:
- optimization of modes after a full dmrg sweep, i.e. $dt$ time step, or after several $dt$ time steps
- Ex: evolution of the imbalance $\Delta N(t) = (N_{\mathrm{even}}(t) - N_{\mathrm{odd}}(t))/N$. in 1D spinless Hubbard model, $|\psi(0)\rangle = |101010\ldots\rangle$

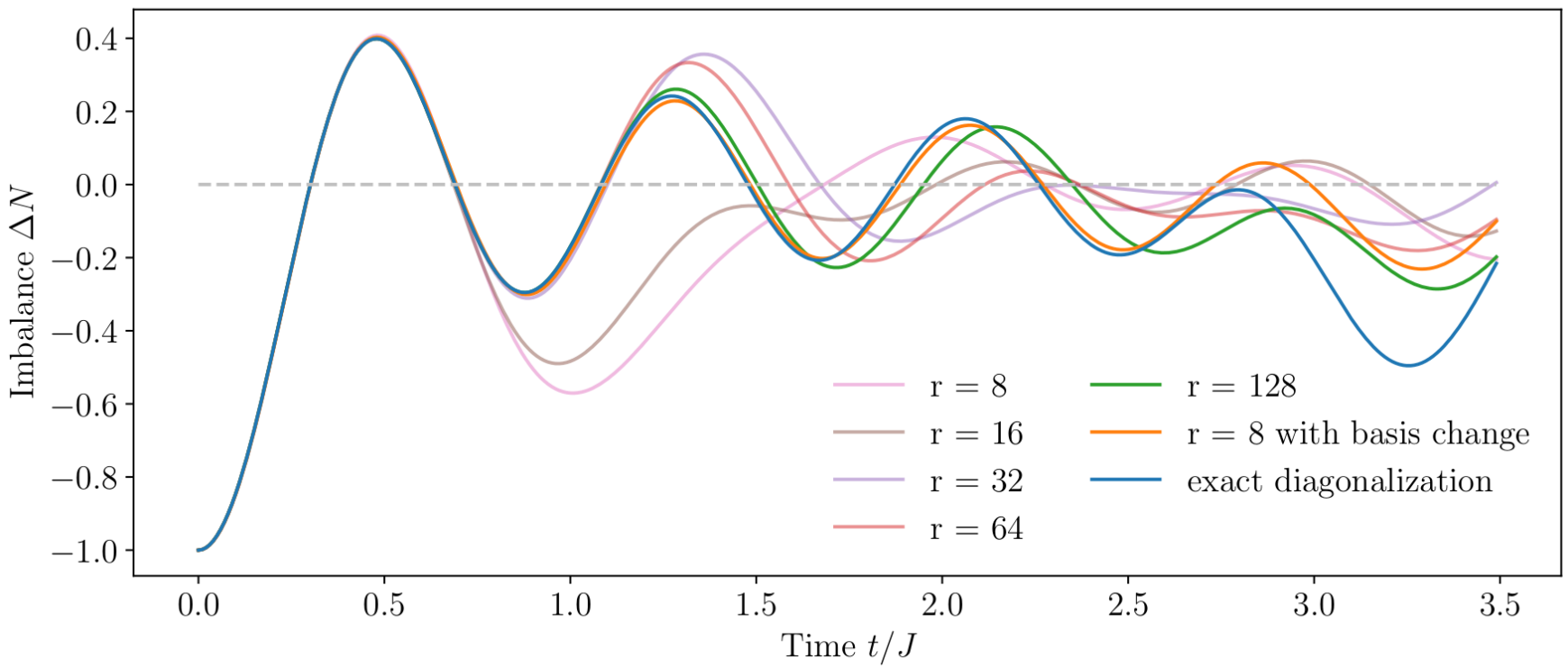

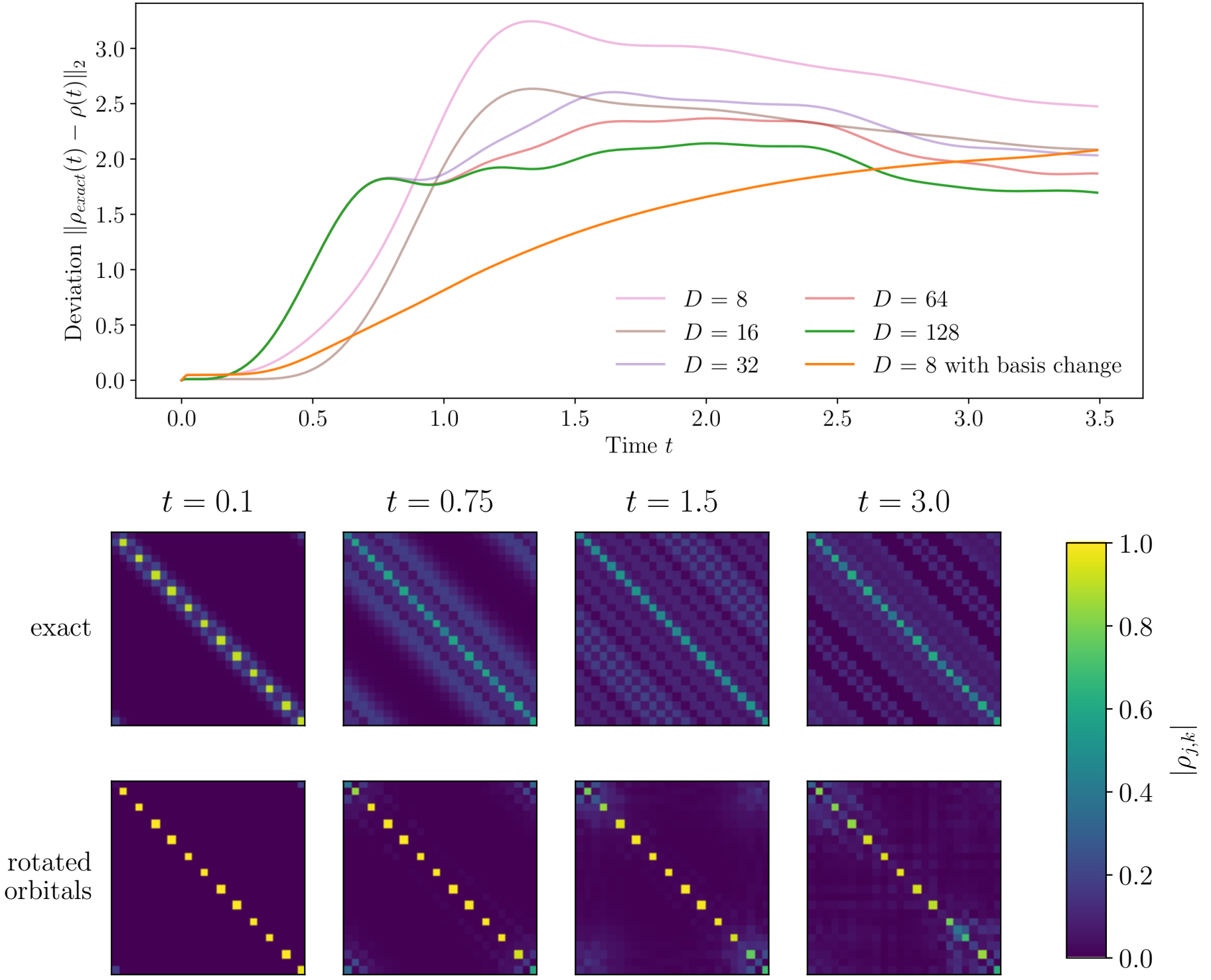
Deviation $\|\rho_{exact}(t) - \rho(t)\|_2$
Time $t$
$D = 8$
$D = 16$
$D = 32$
$D = 64$
$D = 128$
$D = 8$ with basis change
$t = 0.1$
$t = 0.75$
$t = 1.5$
$t = 3.0$
exact
rotated orbitals
$|\rho_{j,k}|$

# Coupled cluster method with single and double excitations tailored by matrix product state wave functions

Kinoshita, Hino, Bartlett, JCP (2005), Veis, Antalik, Neese, Ö.L., Pittner (2016)

- Formally single reference theory, Fermi vacuum is a single determinant
- Split-amplitude ansatz

$$|\Psi_{\mathrm{TCC}}\rangle = e^{\mathcal{T}} |\Psi_{\mathrm{ref}}\rangle = e^{\mathcal{T}^{\mathrm{ext}}+\mathcal{T}^{\mathrm{CAS}}} |\Psi_{\mathrm{ref}}\rangle$$

- $\mathcal{T}^{\mathrm{CAS}}$
  - amplitudes extracted from DMRG (CASCI) calculation
  - frozen during CC calculation
  - account for static correlation
- $\mathcal{T}^{\mathrm{ext}}$
  - determined through the usual CC
  - account for dynamic correlation

$$\begin{aligned} |\Psi_{\mathrm{TCCSD}}\rangle &= e^{\left(\mathcal{T}_1^{\mathrm{ext}}+\mathcal{T}_2^{\mathrm{ext}}\right)} e^{\left(\mathcal{T}_1^{\mathrm{CAS}}+\mathcal{T}_2^{\mathrm{CAS}}\right)} |\Psi_{\mathrm{ref}}\rangle \\ &\approx e^{\left(\mathcal{T}_1^{\mathrm{ext}}+\mathcal{T}_2^{\mathrm{ext}}\right)} |\Psi_{\mathrm{CASCI}}\rangle \end{aligned}$$

- Requires only small modifications of the CC code

# Chromium dimer – correlation energies

- Single-point calculation at 1.5 Å
- One-particle basis: RHF with Ahlrichs' SV basis set $\rightarrow$ (48e,42o)
- DMRG space selected based on $S^{(1)}$ profile
- DMRG performed with DBSS ($\epsilon_{\mathrm{tr}} \approx 10^{-7}$)
- Extrapolated DMRG by Olivares-Amaya et al. JCP 142, 034102, 2015 serves as a FCI benchmark

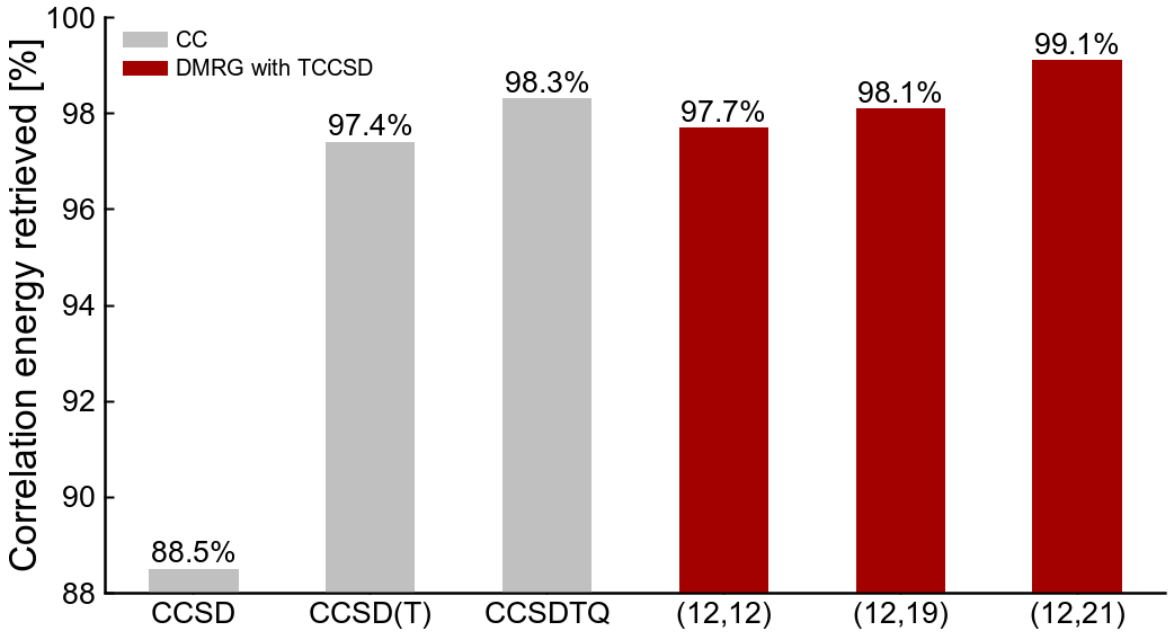


• DMRG-TCC has a quadratic error bound, Faulstich, Laestadius, Ö.L., Schneider, Kvaal(2019) but optimal CAS-EXT split only numerically

• Extensions: similarity transformed TCCSD, LPNO-TCCSD, 4c-DMRG-TCCSD, excited states.

# Ab initio theory of negatively charged boron vacancy qubit in hBN Ivády, Barcza, Thiering,Li, Hamdi, Chou, Ö.L., Gali (2019)

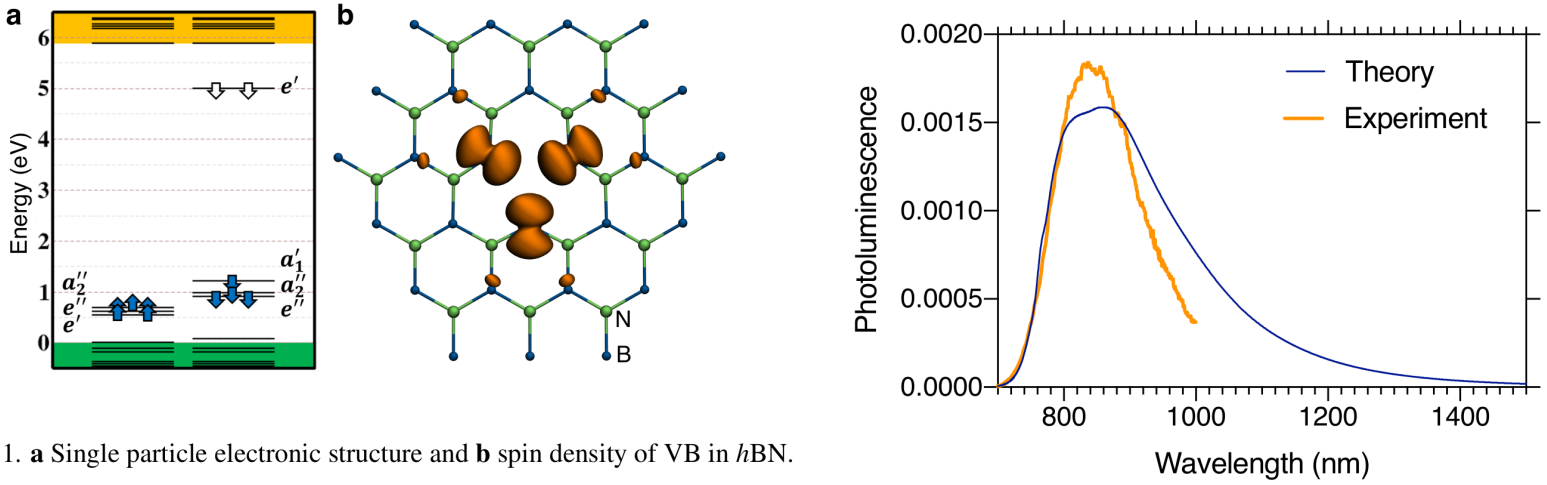


FIG. 1. **a** Single particle electronic structure and **b** spin density of VB in *h*BN.

- Novel combiation of DFT and DMRG for extended systems to treat excited states
- DMRG on top of plane-wave Kohn-Sham orbitals
- ab initio results explain magneto-optical properties of VB in hBN.

Highly tunable magneto-optical response from MgV color centers in diamond Pershin, Barcza, Ö.L., Gali (2021)

- Potential of magnesium-vacancy (MgV) in diamond to operate as a qubit by computing the key electronic and spin properties with robust theoretical methods: Unprecedented control over the magneto-optical response from a qubit by modulating the operational conditions.

# MPS and TNS on kilo-processor architectures:

Nemes, Barcza, Nagy, Ö.L., Szolgay, 2014

- The most time-dominant step of the diagonalization can be expressed as a list of dense matrix operations
- A smart hybrid CPU-GPU implementation, which exploits the power of both CPU and GPU and tolerates problems exceeding the GPU memory size.
- A new CUDA kernel has been designed for asymmetric matrix-vector multiplication to accelerate the diagonalization
- Example: Hubbard model on Intel Xeon E5-2640 2.5GH CPU + NVidia K20 GPU:

1071 GFlops and
$\times 3.5$ speedup is reached.
(Theoretical maximum is
1.17 TFlops)

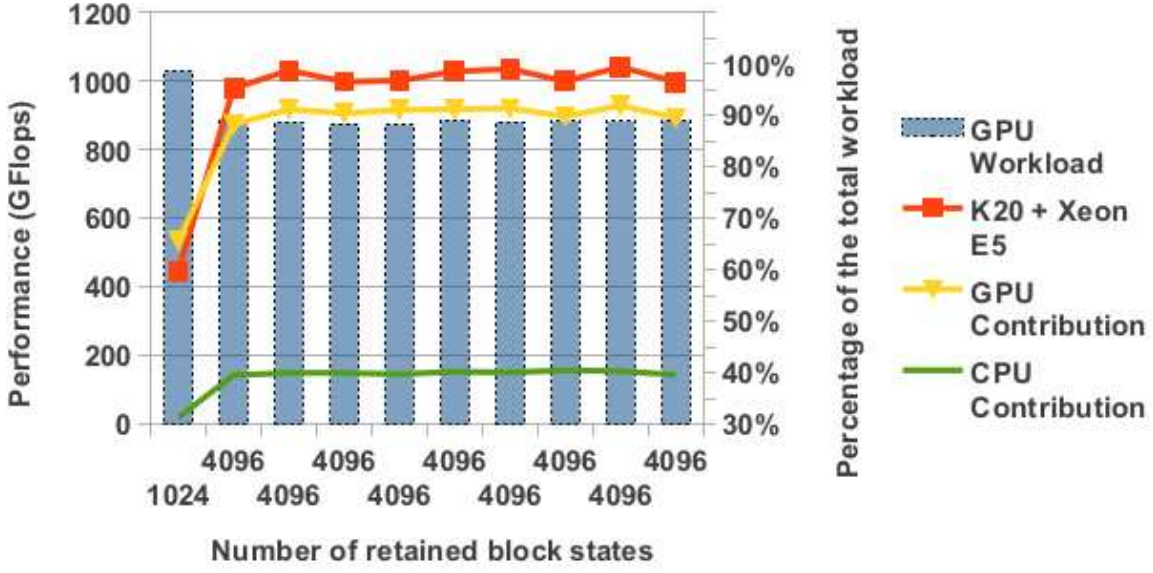

# Massive Parallelization

## J Brabec, J. Brandejs, K. Kowalski, S. Xanntheas, Ö.L., L. Veis (2020)

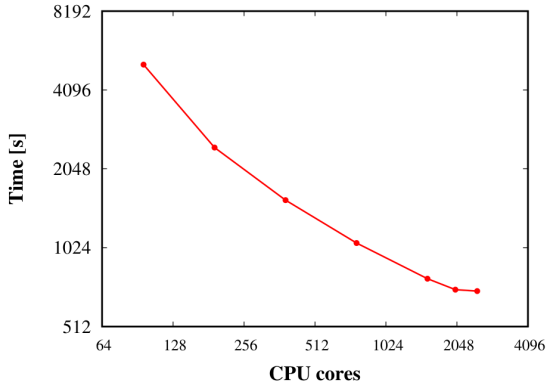


(a) Davidson procedure

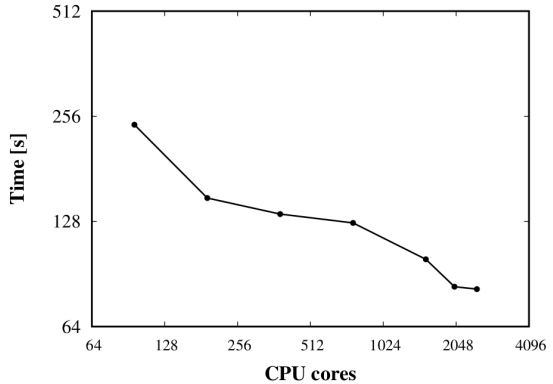


(b) Renormalization

Figure 6: Timings of the Davidson procedure and the renormalization of the QC-DMRG iteration corresponding to the middle of the sweep performed on the Fe(II)-porphyrin model [CAS(32,34)] with bond dimension $M = 8192$.

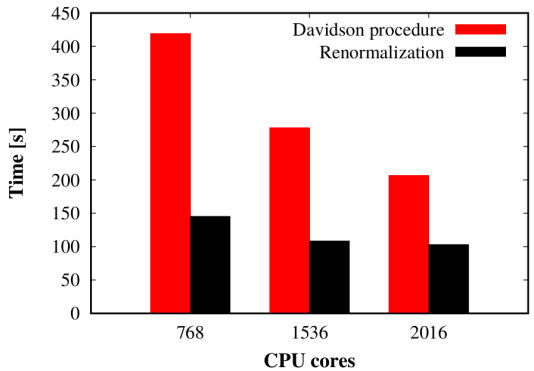


Figure 7: Timings of the Davidson procedure and the renormalization of the QC-DMRG iteration corresponding to the middle of the sweep performed on the defected $\pi$-conjugated anthracene tetramer [CAS(63,63)] with bond dimension $M = 4096$.

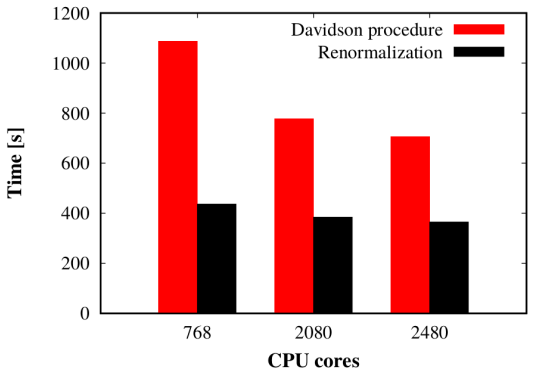


Figure 8: Timings of the Davidson procedure and the renormalization of the QC-DMRG iteration corresponding to the middle of the sweep performed on the FeMoco cluster [CAS(113,76)] with bond dimension $M = 6000$.

# Conclusion

- Tensor topologies together with proper basis representations are important for efficient data sparse representaion of the wavefunction
- Local mode transformation: MPS/TNS based black-box tool to improve basis
- Long time evolution with adaptive mode transformation is a promising direction
- Combination of TNS with other (conventional) methods can exploit benefits of the individual methods
- Massive Parallelization
- $\rightarrow$ Simulation of realistic material properties

Supports: Lendület grant, Hungarian Academy of Sciences, the Hungarian National Research, Development and Innovation Office , Hungarian Quantum Technology National Excellence Program, European Research Area(ERA), DFG, EU (SIQS, RAQUEL, AQUS),the BMBF, and the Studienstiftung des Deutschen Volkes, Grant Agency of the Czech Republic